An Ab Initio Linear Response Method for Computing Magnetic Circular Dichroism Spectra with Non-Perturbative Treatment of Magnetic Field

Shichao Sun, David B. Williams-Young, and Xiaosong Li*

Department of Chemistry, University of Washington, Seattle, WA, 98195

E-mail: xsli@uw.edu

Abstract

Magnetic circular dichroism (MCD) experiments provide a sensitive tool for exploring geometric, magnetic, and electronic properties of chemical complexes and condensed matter systems. They are also challenging to simulate because of the need to simultaneously treat the perturbations of a finite magnetic field as well as an optical field. In this work, we introduce an *ab initio* approach that treats external magnetic field non-perturbatively with London orbitals for simulating the MCD spectra of closed-shell systems. Effects of a magnetic field are included variationally in the spin-free non-relativistic Hamiltonian, followed by a linear response formalism to directly calculate the difference in absorption between the left and right circularly polarized light. In addition to the presentation of underlying mathematical formalism and implementation, the method developed in this paper has been applied to simulations of MCD spectra of the sodium anion, 2,2,6,6-tetramethylcyclohexanone, and 3-methyl-2-hexanone. Results are discussed and compared to experiments.

1 Introduction

Magnetic circular dichroism (MCD) is an important class of magneto-optical spectroscopy in which the probing field is a circularly polarized optical light in the presence of a static magnetic field.[1] The application of a magnetic field couples the (spin and/or orbital) angular momentum of the system to the field. This affects both the positions and intensities of peaks in the electronic spectrum: the former due to an energy shift of each electronic state, and the latter due to perturbations to the wavefunction. This often leads to a breaking of degeneracies and allows for the in-depth spectroscopic study of the fine structure of material systems. Excitingly, because optically active ("bright") and inactive ("dark") states can be coupled together, spectroscopic methods performed in a magnetic field can probe quantum states that are otherwise inaccessible at zero field. Because MCD experiments provide a sensitive tool for exploring geometric, magnetic, and electronic properties of chemical complexes and condensed matter systems, they are widely used in chemistry, biology, and materials research.

Interpreting and understanding MCD spectra has been traditionally based on the first-order perturbative model,[2–6]

$$\frac{\Delta A'}{\mathscr{E}} = \Gamma \mu_B B \sum_J \left[\mathscr{A}_J \left(-\frac{\partial f(\hbar\omega - \hbar\omega_{0J})}{\partial \hbar\omega} \right) + \left(\mathscr{B}_J + \frac{\mathscr{C}_J}{kT} \right) f(\hbar\omega - \hbar\omega_{0J}) \right] \tag{1}$$

$\mathscr{A}_J$ term, which has a derivative band-shape, arises when the degenerate excited states are split due to Zeeman effect. Perturbation of the transition dipole gives rise to $\mathscr{B}_J$ term, which is the most common effect in MCD. The $\mathscr{C}_J$ term is modulated by the Boltzmann distribution of the ground state when degenerate ground states are split by Zeeman effects. The $\mathscr{B}_J$ term is relatively weak compared to the $\mathscr{A}_J$ and $\mathscr{C}_J$ terms, as such it will only be obvious when there are no $\mathscr{A}_J$ and $\mathscr{C}_J$ term contributions, *e.g.*, in a low symmetry closed shell molecule.

Over the past two decades, there have been many successful developments to compute MCD spectra in the perturbative regime, including single residue of the quadratic response

function;[7] the complex polarization propagator method;[8–10] a sum-over-states expression using truncated configuration interaction, with perturbative treatment of the magnetic field and spin-orbit coupling;[11,12] magnetically perturbed time-dependent density functional theory (TDDFT);[13–15] and multi-configurational self-consistent-field with quasi-degenerate perturbation theory to include Zeeman effects with spin-couplings.[16–18] In addition, solvent effects on MCD spectra are also considered.[19,20] Using London orbitals to remove the gauge-dependence of finite atom-centered basis set has been applied in the perturbative calculations of MCD at the level of coupled-cluster,[21,22] Hartree-Fock, and DFT.[23,24]

To the best of our knowledge, there are only two approaches to compute the MCD terms with *variational* treatment of magnetic field. Linderberg and coworkers used the random-phase-approximation (RPA) in the presence of a static magnetic field with semi-empirical evaluation of London orbital integrals to simulate the MCD $\mathscr{B}$ term.[25] Bertsch and coworkers included the orbital Zeeman effect in the local-density-approximation (LDA) using RT–TDDFT integrated over a spatial grid to simulate $\mathscr{A}$- and $\mathscr{B}$-term contributions.[26]

For many-atom systems, electronic structure calculations in the presence of electromagnetic fields become unphysically dependent on the choice of the arbitrary gauge-origin. This is due to the use of atomic-centered orbitals, basis set incompleteness, and truncated expansion of the field-matter interaction, *i.e*, physical observables become dependent on the origin of the electromagnetic field.[27–34] Among various approaches to correct for the gauge-origin problem, electronic structure methods using London type orbitals[35,36] provide the most satisfactory solution.[37–42]

In the perturbative treatment of magnetic field effects, explicit electron integrals of London orbitals are not necessary. However, in the non-perturbative variational approach, complex-valued London orbital integrals must be explicitly evaluated in order to remove the gauge-origin dependence. General recursion relationships for one- and two-electron integrals using London orbitals were pioneered by Helgaker and were recently implemented in the complex generalized Hartree-Fock framework.[43–47]

In this work, we introduce an *ab initio* approach that treats external magnetic field non-perturbatively with London orbitals for simulating MCD spectra of closed-shell systems. This method can describe $\mathscr{A}$ and $\mathscr{B}$ term contributions to the MCD spectrum in a uniform way. Effects of a magnetic field are included variationally in the spin-free non-relativistic Hamiltonian, followed by a linear response theory to obtain the MCD spectrum using a formalism that directly computes the difference of absorption between left- and right-circularly polarized light.

2 Methodology

2.1 MCD Hamiltonian of a Closed-Shell System

In order to simulate MCD spectra, the fundamental Hamiltonian needs to address perturbations from both a static magnetic field and an oscillating optical field. In the non-relativistic framework, the interaction of an electron with external fields in an MCD experiment can be described by the following one-electron Hamiltonian. In this work, we focus on MCD spectra of closed-shell molecular systems, therefore, the spin-Zeeman contributions do not enter the Hamiltonian.

$$h = \frac{1}{2}(\mathbf{p} + \mathbf{A})^2 - U + V \tag{2}$$

$$= -\frac{1}{2}\boldsymbol{\nabla}^2 + \frac{1}{2}(-i\mathbf{r} \times \nabla) \cdot \mathbf{B}_M + \frac{1}{8}(\mathbf{B}_M \times \mathbf{r})^2 + \sum_A \frac{Z_A}{|\mathbf{r} - R_A|}$$

$$- U_W + \mathbf{A}_W \cdot \mathbf{p} + \frac{1}{2}\mathbf{A}_W^2 + \mathbf{A}_W \cdot \mathbf{A}_M \tag{3}$$

where $\mathbf{A}$ and U are the total vector potential and scalar potential of the external fields, respectively. $\mathbf{p} = -i\boldsymbol{\nabla}$ is the momentum operator and V is the nuclear attraction potential. The total vector potential $\mathbf{A}$ includes an applied static magnetic field and a probing optical field (or a plane wave), $\mathbf{A} = \mathbf{A}_M + \mathbf{A}_W$. Since $U_M = 0$ for a static magnetic field, only

the scalar potential of the probing plane wave remains in Eq. (3). We used the relationship between the vector potential and the static magnetic field ($\mathbf{B}_M$), $\mathbf{A}_M = \frac{1}{2}\mathbf{B}_M \times \mathbf{r}$.

Using the electric-dipole approximation in the length gauge for the interaction between the system and the probing plane wave and the relationship $\mathbf{E}_W(\mathbf{r},t) = -\boldsymbol{\nabla} U_W(\mathbf{r},t) - \frac{\partial}{\partial t}\mathbf{A}_W(\mathbf{r},t)$, the final working Hamiltonian for simulating MCD experiment is:

$$h = -\frac{1}{2}\boldsymbol{\nabla}^2 + \frac{1}{2}(-i\mathbf{r}\times\nabla)\cdot\mathbf{B}_M + \frac{1}{8}(\mathbf{B}_M\times\mathbf{r})^2 + \sum_A \frac{Z_A}{|\mathbf{r}-R_A|} - \mathbf{r}\cdot\mathbf{E}_W \tag{4}$$

Note that in Eq. (4), higher order perturbations arising from interactions between the electronic system and the probing optical field, such as the electric-quadrupole and magnetic-dipole terms, are ignored.

In the following discussion, we remove the subscript notations "M" and "W" for simplicity, however, readers should keep in mind that $\mathbf{B}$ and $\mathbf{E}$ fields originate from two different external perturbations.

The second term in Eq. (4) includes orbital Zeeman contributions, and the third term is the diamagnetic contribution. The diamagnetic term is quadratic in the strength of the magnetic field, which can be expanded as

$$\begin{aligned}(\mathbf{B}\times\mathbf{r})^2 =& (B_y^2+B_z^2)x^2 + (B_x^2+B_z^2)y^2 + (B_x^2+B_y^2)z^2 \\ &- 2B_xB_yxy - 2B_yB_zyz - 2B_xB_zxz\end{aligned} \tag{5}$$

This $\mathbf{B}^2$ term plays an important role in molecular diamagnetism, especially in large magnetic fields and in closed-shell systems.

The total one-electron Hamiltonian Eq. (4) can be separated as $h(t) = h_0 + V(t)$, where the time-dependent perturbation, $V(t) = -\mathbf{r}\cdot\mathbf{E}(t)$, is the electric-dipole interaction, and h_0

is the time-independent reference Hamiltonian,

$$h_0 = -\frac{1}{2}\boldsymbol{\nabla}^2 + \frac{1}{2}(-i\mathbf{r}\times\nabla)\cdot\mathbf{B}_M + \frac{1}{8}(\mathbf{B}_M\times\mathbf{r})^2 + \sum_A \frac{Z_A}{|\mathbf{r}-R_A|} \tag{6}$$

The separation of time-dependent and time-independent contributions to the total Hamiltonian allows different procedures to treat the separate external perturbations in an MCD calculation. Instead of using perturbative treatments for both the static magnetic and oscillating optical fields, we introduce a semi-variational approach in which the wave function is variationally optimized in the presence of a static magnetic field (Sec. 2.2) and the response to the oscillating circularly polarized optical field is taken at the weak-field limit (Sec. 2.3).

2.2 Ground State with Variational Treatment of Magnetic Field using London Orbitals

In the numerical implementation developed in this work, the Hamiltonian is cast in an atomic basis. In restricted Hartree-Fock, the molecular orbitals $\{\phi_j(\mathbf{r})\}$ are expanded in terms of a set of complex London orbitals $\{\tilde{\chi}_\mu(\mathbf{r},\mathbf{k}_A)\}$,

$$\phi_j(\mathbf{r}) = \sum_\mu C_{\mu j}\tilde{\chi}_\mu(\mathbf{r},\mathbf{k}_A) \tag{7}$$

$$\tilde{\chi}_\mu(\mathbf{r},\mathbf{k}_A) = \chi_\mu(\mathbf{r}-\mathbf{R}_A)e^{i\mathbf{k}_A\cdot(\mathbf{r}-\mathbf{R}_A)} \tag{8}$$

where $\{\chi_\mu(\mathbf{r}-\mathbf{R}_A)\}$ are real Gaussian type atomic orbital (AO) basis functions centered at $\mathbf{R}_A$. The exponential form of the London orbital phase factor defines the local gauge origin at each nuclear center in the presence of magnetic field with a plane wave vector described by $\mathbf{k}_A = \frac{\mathbf{R}_A\times\mathbf{B}}{2}$, where $\mathbf{B}$ is the external magnetic field.

The one-electron integral for any one-electron operator $\hat{O}_1$ with London orbitals can be

defined as

$$O_{1,\mu\nu} = (\mu|O_1|\nu) = \int \mathrm{d}^3\mathbf{r}\tilde{\chi}^*_\mu(\mathbf{r},\mathbf{k}_A)\,\hat{O}_1\,\tilde{\chi}_\nu(\mathbf{r},\mathbf{k}_B) = \int \mathrm{d}^3\mathbf{r}\tilde{\chi}_\mu(\mathbf{r},-\mathbf{k}_A)\,\hat{O}_1\,\tilde{\chi}_\nu(\mathbf{r},\mathbf{k}_B) \tag{9}$$

and the electron repulsion integrals (ERIs) are,

$$(\mu\nu|\kappa\lambda) = \int \mathrm{d}^3\mathbf{r}_1 \int \mathrm{d}^3\mathbf{r}_2 \frac{\tilde{\chi}^*_\mu(\mathbf{r}_1,\mathbf{k}_A)\tilde{\chi}_\nu(\mathbf{r}_1,\mathbf{k}_B)\tilde{\chi}^*_\kappa(\mathbf{r}_2,\mathbf{k}_C)\tilde{\chi}_\lambda(\mathbf{r}_2,\mathbf{k}_D)}{|\mathbf{r}_1-\mathbf{r}_2|} \tag{10}$$

In a perturbative treatment of the static magnetic field, explicit electron integrals using London orbitals with a finite field are not needed.[21–24] However, for the variational approach, complex-valued London orbital integrals must be evaluated. For details on integral evaluation using London orbitals, we refer readers to Refs. 43,45,47. Integrals are evaluated in complex arithmetic, implemented in the Chronus Quantum software package.[48]

Using the formalism of restricted Hartree-Fock for closed-shell systems, the time-independent Fock matrix can be written as,

$$\begin{aligned}\mathbf{F}_0 = \quad & \mathbf{T}+\mathbf{V}+\mathbf{J}[\mathbf{P}_0]-\frac{1}{2}\mathbf{K}[\mathbf{P}_0]-\frac{i}{2}\mathbf{L}\cdot\mathbf{B} \\ & +\frac{1}{8}\big\{(B_y^2+B_z^2)\mathbf{q}_{xx}+(B_x^2+B_z^2)\mathbf{q}_{yy}+(B_x^2+B_y^2)\mathbf{q}_{zz} \\ & -2B_xB_y\mathbf{q}_{xy}-2B_yB_z\mathbf{q}_{yz}-2B_xB_z\mathbf{q}_{xz}\big\}\end{aligned} \tag{11}$$

where $\mathbf{L}_{\mu\nu} = (\tilde{\chi}_\mu|\mathbf{r}\times\boldsymbol{\nabla}|\tilde{\chi}_\nu)$ is the orbital-angular momentum integral , and $(\mathbf{q}_{nm})_{\mu\nu} = (\tilde{\chi}_\mu|\hat{r}_n\hat{r}_m|\tilde{\chi}_\nu)$ is the electric quadrupole integral. The density matrix is defined as

$$P_{0,\mu\nu} = 2\sum_i^{N/2} C_{\mu i}C^*_{\nu i} \tag{12}$$

where N is the number of electrons.

The Coulomb (**J**) and exchange (**K**) matrix elements are,

$$J_{\mu\nu}[\mathbf{P}_0] = \sum_{\lambda\kappa}(\mu\nu|\kappa\lambda)P_{0,\lambda\kappa} \tag{13}$$

$$K_{\mu\nu}[\mathbf{P}_0] = \sum_{\lambda\kappa}(\mu\lambda|\kappa\nu)P_{0,\lambda\kappa} \tag{14}$$

Because the fundamental electron integrals are complex-valued, in this work, we use complex restricted Hartree-Fock (ℂ-RHF) as our reference. Note that since ERIs using London orbitals are complex-valued, they only have a four-fold symmetry instead of eight, as in the case of real-valued ERIs,

$$(\mu\nu|\kappa\lambda) =(\kappa\lambda|\mu\nu) = (\nu\mu|\lambda\kappa)^* = (\lambda\kappa|\nu\mu)^* \tag{15}$$

2.3 Perturbation of Left/Right Circularly Polarized Light

In this work, we only consider the electric-dipole contribution to the MCD spectrum (Eq. (4)). Higher order multipole moment contributions, such as electric-quadrupole and magnetic-dipole arising from the system-light interaction, are ignored.

In an MCD experiment, the direction of magnetic field is usually made parallel to the propagation direction of incident light. Defining the direction of the incident light as γ, where γ can be $\{x, y, z\}$, the circularly polarized dipoles are

$$\mu_\gamma^- = \frac{1}{\sqrt{2}}(\mu_\alpha - i\mu_\beta) \tag{16}$$

$$\mu_\gamma^+ = \frac{1}{\sqrt{2}}(\mu_\alpha + i\mu_\beta) \tag{17}$$

where $\{\alpha, \beta, \gamma\} \equiv \{x, y, z\}$, $\{y, z, x\}$ or $\{z, x, y\}$, following the right hand rule. The difference

of absorbance between left- and right-polarized light per photon energy can be written as

$$\frac{\Delta A'}{\mathscr{E}} = \frac{\epsilon'_- - \epsilon'_+}{\mathscr{E}} d\ l = \Gamma \sum_J \sum_\gamma \frac{1}{3} (|\left\langle 0 \left| \mu_\gamma^- \right| J \right\rangle'|^2 - |\left\langle 0 \left| \mu_\gamma^+ \right| J \right\rangle'|^2) f(\hbar\omega - \hbar\omega'_{0J}) \tag{18}$$

where primed notations refer to quantities calculated in the presence of a static magnetic field, $\mathscr{E} = \hbar\omega$ is the energy per photon, d is concentration of solution in mol/L, l is the length of the path through the sample in centimeters,[4] γ is the direction of propagation of incident photon, $f(\hbar\omega - \hbar\omega'_{0J})$ is the band shape function, and $\hbar\omega'_{0J}$ is the excitation energy from ground state to the excited state J in the presence of a static magnetic field. Note that Eq. (18) takes on an isotropic average of all directions of incident light and applied magnetic field where the summation of γ runs over x, y, z. The derivation of the rotational average can be found in Reference 4.

Γ is the a collection of physical constants defined as[4]

$$\Gamma = \frac{N_0 \pi^2 \alpha^2 d\ l\ \log_{10} e}{250\ \hbar\ c\ n} \tag{19}$$

where α is the permittivity and n is the index of refraction.

The difference between oscillator strengths of left- and right-circularly polarized light for excited state J can be written as:[4]

$$\sum_\gamma (|\left\langle 0 \left| \mu_\gamma^- \right| J \right\rangle'|^2 - |\left\langle 0 \left| \mu_\gamma^+ \right| J \right\rangle'|^2) = i \sum_{\alpha\beta\gamma} \epsilon_{\alpha\beta\gamma} \left\langle 0 \left| \mu_\alpha \right| J \right\rangle^\gamma \left\langle J \left| \mu_\beta \right| 0 \right\rangle^\gamma \tag{20}$$

where $\epsilon_{\alpha\beta\gamma}$ is Levi-Civita symbol ($\epsilon_{xyz} = \epsilon_{yzx} = \epsilon_{zxy} = 1$, $\epsilon_{yxz} = \epsilon_{xzy} = \epsilon_{zyx} = -1$, otherwise 0). We use superscript γ to explicitly denote the direction of the applied magnetic field.

Substituting Eq. (20) in Eq. (18), we reach the working formalism for computing MCD spectra,

$$\frac{\Delta A'}{\mathscr{E}} = \Gamma \sum_J \frac{1}{3} \left(i \sum_{\alpha\beta\gamma} \epsilon_{\alpha\beta\gamma} \left\langle 0 \left| \mu_\alpha \right| J \right\rangle^\gamma \left\langle J \left| \mu_\beta \right| 0 \right\rangle^\gamma \right) f(\hbar\omega - \hbar\omega_{0J}^\gamma) \tag{21}$$

Compared to the conventional definition of the $\mathscr{B}$ term in perturbation theory, one can define the MCD strength of excited state $|J\rangle$ as

$$R_J = \frac{i}{3} \frac{\sum_{\alpha\beta\gamma} \epsilon_{\alpha\beta\gamma} \langle 0 | \mu_\alpha | J \rangle^\gamma \langle J | \mu_\beta | 0 \rangle^\gamma}{\mu_B |\mathbf{B}|} \tag{22}$$

where μ_B is Bohr magneton. If the magnetic field does not split excited states of different M_L that belong to a same orbital angular momentum quantum number, the first order approximation of R_J becomes $\mathscr{B}_J$ in the perturbative treatment. The MCD strength (Eq. (22)) is written in atomic units, whereas the conventional experimentally reported unit is $D^2 \cdot \mathrm{cm}$, where D is Debye.[4] The conversion for R_J from atomic units to the conventional unit of $D^2 \cdot \mathrm{cm}$ is 1 a.u. $= 2.944 \times 10^{-5} D^2 \cdot \mathrm{cm}$.

The perturbative approach (Eq. (1)) is formulated in terms of the state-specific field-free parameters $\mathscr{A}_J, \mathscr{B}_J, \mathscr{C}_J$. In contrast, Eq. (21) directly computes MCD observables using a variational treatment of the external finite magnetic field. Compared to the perturbative approach, the expression in Eq. (21) contains $\mathscr{A}_J$ and $\mathscr{B}_J$ terms, and their higher order contributions.

Without an applied magnetic field, the absorbance difference between left- and right-circularly polarized light is zero for electric circular dichroism (ECD) inactive molecules (or natural optical inactive molecules). In the presence of a static magnetic field, the imaginary part of transition dipole ($\langle 0 | \mu_\alpha | J \rangle^\gamma$ and $\langle 0 | \mu_\alpha | J \rangle^\gamma$) has nonzero contribution to the MCD strength,[1] which can be understood directly from Eq. (21). Since the excitation energy ω^γ is computed in the presence of a magnetic field, the breaking of excited state degeneracies, *i.e.* the $\mathscr{A}_J$ term, as a result of orbital Zeeman and diamagnetic effects are also included in Eq. (21). For closed-shell molecules, there is no spin degeneracy in the unperturbed ground state. In addition, the optical gap of a molecular system is usually larger than $k_B T$, where k_B is the Boltzmann constant. As a result, almost all molecules are in the ground state in experimental temperature, and thus the equivalent $\mathscr{C}$ term contribution can be ignored.

The computational approach introduced here (Eq. (21)) has a unique advantage that it only requires the computation of a single response to external optical perturbation due to the variational treatment of a finite magnetic field in the reference state. In contrast, perturbative approaches, such as the sum-over-states expression, require computations of all excited states.[9,49] Complex polarization propagator methods[8,10] need to numerically resolve quadratic response functions at different frequencies, but can be advantageous in the high density-of-state region. Alternatively, $\mathscr{A}_J$ and $\mathscr{B}_J$ terms can be computed via the evaluation of the derivatives of transition density and excitation energy with respect to magnetic perturbation.[14,15]

2.4 Linear Response ℂ-TDHF

In order to compute MCD spectra using Eq. (21), electronic optical excitations need to be computed in the presence of a finite magnetic field. In this work, this is achieved using the linear response complex time-dependent Hartree-Fock (ℂ-TDHF) approach. The reference of ℂ-TDHF is the solution of ℂ-HF with the finite magnetic field included variationally.

The working equation of TDHF is given as

$$\begin{pmatrix} \mathbf{A}^\gamma & \mathbf{B}^\gamma \\ \mathbf{B}^{\gamma *} & \mathbf{A}^{\gamma *} \end{pmatrix} \begin{pmatrix} \mathbf{X}^\gamma \\ \mathbf{Y}^\gamma \end{pmatrix} = \omega^\gamma \begin{pmatrix} \mathbf{I} & \mathbf{0} \\ \mathbf{0} & -\mathbf{I} \end{pmatrix} \begin{pmatrix} \mathbf{X}^\gamma \\ \mathbf{Y}^\gamma \end{pmatrix} \tag{23}$$

$$B_{ai,bj} = (ai||bj) \tag{24}$$

$$A_{ai,bj} = (ai||jb) + \delta_{ab}\delta_{ij}(\epsilon_a - \epsilon_i) \tag{25}$$

where γ is the direction of the applied finite magnetic field in the ground state reference. Note, since the GIAO integrals and ℂ-HF are used, matrix elements in Eq. (23) are complex valued.

Given the direction γ of the applied uniform magnetic field, the corresponding transition

dipole can be assembled from the transition density.

$$\langle 0 \left| \mu_\alpha \right| J \rangle^\gamma = \sum_i \sum_a \left(\langle i \left| \mu_\alpha \right| a \rangle^\gamma X^\gamma_{J,ai} + \langle a \left| \mu_\alpha \right| i \rangle^\gamma Y^\gamma_{J,ai} \right), \qquad \mu_\alpha \in \{\mu_x, \mu_y, \mu_z\} \tag{26}$$

where i and a sum over occupied and virtual molecular orbitals (MOs), respectively, and $\langle a \left| \mu_\alpha \right| i \rangle^\gamma$ and $\langle i \left| \mu_\alpha \right| a \rangle^\gamma$ are the dipole integrals in MO basis.

3 Computational Detail

To obtain the transition dipoles required in Eq. (21), three separate linear response ℂ-TDHF calculations were carried out with a magnetic field applied in the x, y, and z directions. Gauge including atomic orbitals (GIAO) were used to eliminate the gauge origin dependence in the variational treatment of the finite magnetic field described in Sec. 2.2. The geometries of molecules were optimized with the B3LYP functional[50–52] with a 6-31G(d) basis set[53,54] without a magnetic field using the GAUSSIAN16 computational chemistry software package.[55] ℂ-TDHF calculations in magnetic field using the GIAO 6-31G(d) basis set were performed in the CHRONUS QUANTUM open source package.[48] Computed spectra are broadened with a normalized Gaussian function.

$$f_J(\omega) = \frac{1}{\sqrt{\pi}\sigma_J} \exp\left[- \left(\frac{\omega - \omega'_J}{\sigma_J} \right)^2 \right] \tag{27}$$

where ω and ω'_J are in atomic units. A major advantage of MCD over absorption spectra of linear polarized light is that MCD can resolve Zeeman effects with a higher resolution. This can be seen via a simple mathematical exercise using Gaussian broadening function, as shown in the Appendix.

4 Benchmark and Discussion

4.1 Sodium Anion

The existence of sodium anion was experimentally confirmed from an MCD measurement, with an absorption peak at ∼600 nm resulting from the $s \rightarrow p$ orbital transition.[56] An external magnetic field introduces orbital Zeeman interactions that break the three-fold degeneracy of the p orbitals, illustrated in Fig. 1. This gives rise to two peaks of opposite sign which leads to a derivative shape, shown in Fig. 2. The effects of magnetic field on the wave functions and properties of the ground and excited states are fully accounted for by treating the magnetic field variationally. As a result, $\mathscr{A}$ and $\mathscr{B}$ terms as well as their higher-order contributions are included in the simulated results. In comparison, it is required by perturbation theory to include infinite orders of magnetic field perturbations to fully describe the effects.

Computed excitation energies and associated MCD strengths are listed in Tab. 1. In this calculation, a magnetic field of 5.0×10^{-5} a.u. (∼11.75 T) was applied and the MCD spectrum was computed using the method introduced here. The relatively large magnitude of the magnetic field is chosen in the calculation to avoid numerical noise and instability. Note that we only present the MCD intensity in arbitrary unit because the concentration, d, and length of the path of light, l, are not defined in the experimental literature. The center of the computed MCD band is located at ∼720 nm. We do not expect a quantitative agreement with the experiment as the experimental conditions are not modeled in this work. Nevertheless, the derivative band-shape of the Na^- MCD spectrum is obtained using the variational method introduced here.

4.2 2,2,6,6-tetramethylcyclohexanone

In the absence of excited state splitting, the main effect of an external magnetic field comes from the perturbed transition dipole moment, giving rise to the perturbation-theory equiv-

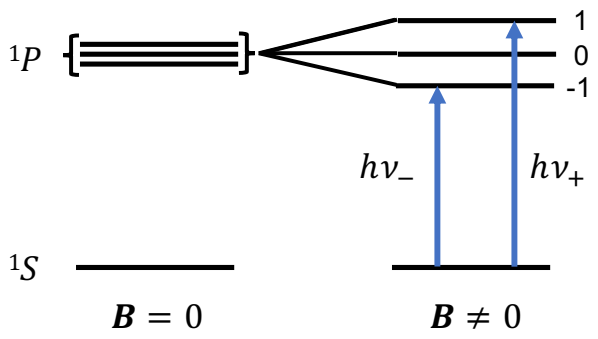

Figure 1. Illustration of splitting of the Na^- $s \rightarrow p$ transition. Without the external magnetic field, the excited states have a three-fold degeneracy. In the presence of a finite magnetic field, excited states of different M_L values split.

Table 1. Excitation energies and MCD strengths of Na^- $s \rightarrow p$ transitions in a 5×10^{-5} a.u. ($\sim$11.75 T) magnetic field.

ω'_{0J}/eV	$R/\times 10^5$ a.u.
1.72587	−11.1937
1.72655	0.0000
1.72723	11.1937

alent $\mathscr{B}_J$ term contribution.

MCD calculation of 2,2,6,6-tetramethylcyclohexanone in a 2.106×10^{-5} a.u. ($\sim$4.95 T) magnetic field is carried out. In order to be consistent with experimental measurements, the computed MCD spectrum is presented as the magnetic-field normalized molar ellipticity, $[\theta]_M$. The calculation of $[\theta]_M$, in the conventional unit of Degree$(\text{mol/L})^{-1}\text{m}^{-1}\text{Gauss}^{-1}$, is $[\theta]_M = 0.0014802 \sum_J R_J \omega f(\hbar\omega - \hbar\omega^{\gamma}_{0J})$ where R_J, ω, and f are computed in atomic units.[14]

The computed MCD spectrum of 2,2,6,6-tetramethylcyclohexanone is shown in Fig. 3, and the associated excitation energy and MCD strength are reported in Tab. 2. The peak at $\sim$4.8 eV is characterized as the $n \rightarrow \pi^*$ transition. Although the computed result is of the correct + sign, the center of the peak is blue-shifted compared to the experimental value of 4.1 eV.[57] In addition, the magnitude of peak intensity is higher than that measured in experiment. This is likely due to the lack of solvent effects and electron correlation in the current work.

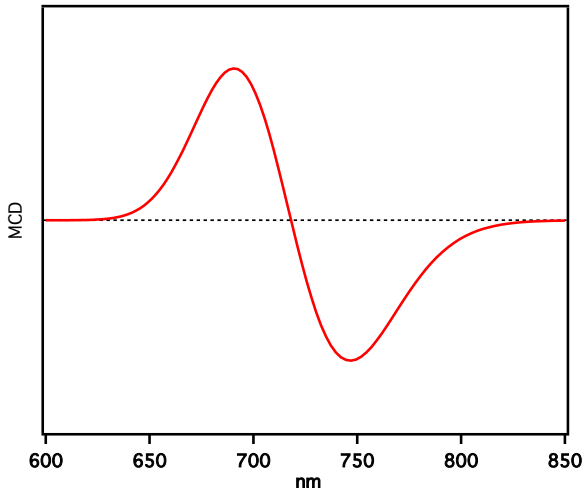

Figure 2. Simulated MCD spectra of Na^- $s \rightarrow p$ transitions in a 5×10^{-5} a.u. ($\sim$11.75 T) magnetic field. An arbitrary unit and Gaussian broadening with $\sigma = 0.035$ are used.

Table 2. Excitation energies and MCD strengths of 2,2,6,6-tetramethylcyclohexanone $n \rightarrow \pi^*$ transition in a 2.106×10^{-5} a.u. ($\sim$4.95 T) magnetic field.

ω'_{0J}/eV	R/a.u.
4.79665719	0.038400153724942

4.3 3-methyl-2-hexanone

For natural optical active molecules, such as (R,S)-3-methyl-2-hexanone shown in Fig. 4.1 and Fig. 4.2,[57] electronic circular dichroism (ECD) spectra can be obtained in the absence of a magnetic field, however, ECD signals disappear if the ensemble consists of equal amounts of R- and S-enantiomers. In this case, MCD spectra are particularly useful as the effect of an external magnetic field can make the MCD signal visible.

Figure 5 shows the simulated MCD spectra of 3-methyl-2-hexanone in a 2.106×10^{-5} a.u. ($\sim$4.95 T) magnetic field and the associated numerical values are reported in Tab. 3. The strength of the magnetic field used is comparable to that used in the experiment.[57] The calculated MCD spectra of (R)- and (S)-3-methyl-2-hexanone are of the same '$-$' sign, in agreement with experiment.[57] As a result, even if the sample consists of equal amounts

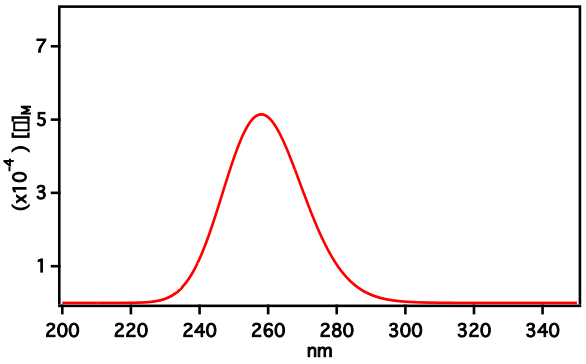

Figure 3. Simulated MCD spectrum of 2,2,6,6-tetramethylcyclohexanone in a 2.106×10^{-5} a.u. ($\sim$4.95 T) magnetic field. Gaussian broadening with $\sigma = 0.011$ is used.

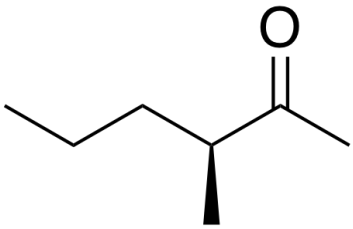

Figure 4.1. Molecular structure of (R)-3-methyl-2-hexanone

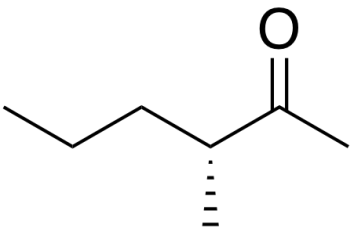

Figure 4.2. Molecular structure of (S)-3-methyl-2-hexanone

of R- and S-enantiomers, one still can measure the MCD signal. The excitation at $\sim$4.97 eV ($\sim$250 nm) arises from the excitation from the lone pair electron of oxygen to the π^* anti-bonding orbital of the CO double bond. The peak position of the calculated spectrum is about 20 nm blue-shifted compared to the experimental value,[57] however, the height of the peak is similar to experiment.

Table 3. Excitation energies and MCD strengths of 3-methyl-2-hexanone in a 2.106×10^{-5} a.u. ($\sim$4.95 T) magnetic field.

ω'_{0J}/eV	R/a.u.
4.96819	-0.002011

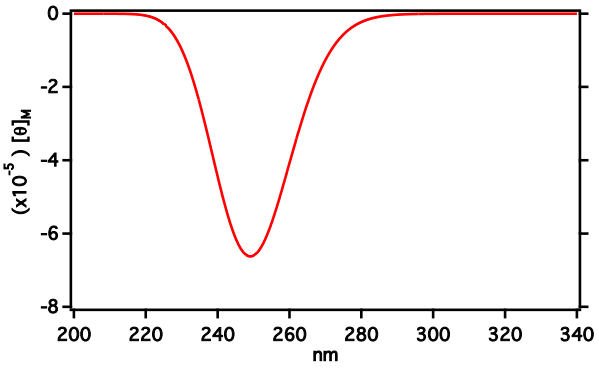

Figure 5. Simulated MCD spectra of 3-methyl-2-hexanone in a 2.106×10^{-5} a.u. ($\sim$4.95 T) magnetic field. Gaussian broadening with $\sigma = 0.011$ is used.

5 Conclusion

In this paper, we presented a mathematical formalism and implementation of an *ab initio* method with non-perturbative treatment of magnetic field for computing magnetic circular dichoism spectra of closed-shell systems. The approach developed in this work utilizes a spin-free non-relativistic Hamiltonian as the ground state reference that variationally includes the effects of a finite magnetic field, including orbital Zeeman and diamagnetic terms. MCD spectra are computed using the linear response formalism and direct calculation of left- and right-circular polarizations. In order to remove the gauge-origin dependence, London orbitals are used explicitly in the non-perturbative treatment of the finite magnetic field.

The method developed in this paper has been applied to simulations of MCD spectra of sodium anion, 2,2,6,6-tetramethylcyclohexanone, and 3-methyl-2-hexanone. Results are discussed and compared to experiments, and all computed benchmark spectra were able to return spectra with the correct sign. Particularly, the derivative band-shape of Na^- MCD spectrum was obtained using the variational method developed here, however, due the lack of electron correlation effect, the computed peak positions are not in good agreement with experiment. Nevertheless, the electronic transition characteristics in an MCD measurement can be correctly obtained at a low computational cost using the method developed in this work.

Acknowledgement

The development of electronic structure method with magnetic field perturbation is funded by the US Department of Energy (DE-SC0006863). The development of non-perturbative spectroscopic methods is supported by the National Science Foundation (CHE-1565520). The development of the Chronus Quantum open source software package is supported by the National Science Foundation (OAC-1663636). David Williams-Young was supported by a fellowship from The Molecular Sciences Software Institute (MolSSI) under NSF grant ACI-1547580. Computations were facilitated through the use of advanced computational, storage, and networking infrastructure provided by the Hyak supercomputer system at the University of Washington, funded by the Student Technology Fee and the National Science Foundation (MRI-1624430).

Appendix – MCD Peak Broadening

We use two peaks close in energy with opposite sign as an example to illustrate the derivative peak profile in an MCD measurement. For example, when p orbitals of different M_L quantum numbers split due to the orbital Zeeman term, two excitations with opposite sign appear in the MCD measurement (Fig. 1). The discussion herein can be extended to other types of Zeeman splitting as well.

The separation of energy is $2\Delta\omega$, which is usually on the order of meV. Assuming a Gaussian broadening, the band shape function of these two peaks can be written as

$$f(x) = Ce^{-\left[\frac{(x+\Delta\omega)}{\sigma}\right]^2} - Ce^{-\left[\frac{(x-\Delta\omega)}{\sigma}\right]^2} \tag{28}$$

where C is normalization constant. The peak positions are the stationary points of function

$f(x)$, where the first derivative of the band is zero:

$$\frac{df}{dx} = \frac{2C}{\sigma^2}\left((x-\Delta\omega)e^{-\left[\frac{(x-\Delta\omega)}{\sigma}\right]^2} - (x+\Delta\omega)e^{-\left[\frac{(x+\Delta\omega)}{\sigma}\right]^2}\right) = 0 \tag{29}$$

The solution of Eq. (29) can be obtained by locating the intersects of the two functions in the following equation, shown in Eq. (30),

$$-\frac{4x\Delta\omega}{\sigma^2} = \ln\frac{x-\Delta\omega}{x+\Delta\omega} \tag{30}$$

Equation (30) shows that the separation between two stationary points are greater than separation between the two excitations ($2\Delta\omega$). A larger Gaussian width σ gives rise to a larger peak separation and a broader profile.

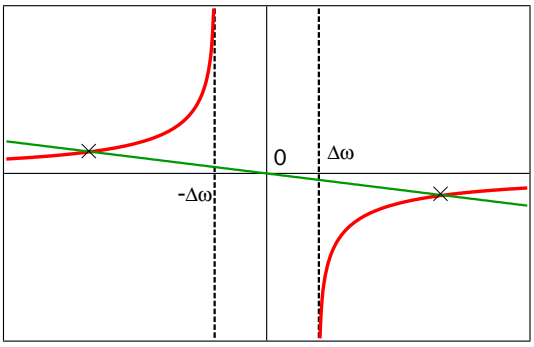

Figure 6. Green and red curves are $y = -\frac{4x\Delta\omega}{\sigma^2}$ and $y = \ln\frac{x-\Delta\omega}{x+\Delta\omega}$. Dotted lines are located at $x = +\Delta\omega$ and $x = -\Delta\omega$. Positions where $-\frac{4x\Delta\omega}{\sigma^2}$ intersects, $\ln\frac{x-\Delta\omega}{x+\Delta\omega}$, are marked with an $\times$.

References

(1) Barron, L. D. *Molecular Light Scattering and Optical Activity*; Cambridge University Press: New York, 2009.

(2) Buckingham, A.; Stephens, P. Magnetic Optical Activity. *Annu. Rev. Phys. Chem.* **1966**, *17*, 399–432.

(3) Solomon, E.; Neidig, M.; Schenk, G. In *Comprehensive Coordination Chemistry II: from Biology to Nanotechnology*; McCleverty, J. A., Meyer, T. J., Eds.; Elsevier Pergamon: Amsterdam, 2003; Chapter 2.26, pp 339–349.

(4) Piepho, S. B.; Schatz, P. N. *Group Theory in Spectroscopy: with Applications to Magnetic Circular Dichroism*; Wiley-Interscience, 1983; Vol. 1.

(5) Mason, W. R. *A Practical Guide to Magnetic Circular Dichroism Spectroscopy*; John Wiley & Sons, Inc: Hoboken, New Jersey, 2006.

(6) Kjærgaard, T.; Coriani, S.; Ruud, K. Ab Initio Calculation of Magnetic Circular Dichroism. *WIREs Comput. Mol. Sci.* **2012**, *2*, 443–455.

(7) Coriani, S.; Jørgensen, P.; Rizzo, A.; Ruud, K.; Olsen, J. Ab Initio Determinations of Magnetic Circular Dichroism. *Chem. Phys. Lett.* **1999**, *300*, 61–68.

(8) Solheim, H.; Ruud, K.; Coriani, S.; Norman, P. Complex Polarization Propagator Calculations of Magnetic Circular Dichroism Spectra. *J. Chem. Phys.* **2008**, *128*, 094103.

(9) Krykunov, M.; Seth, M.; Ziegler, T.; Autschbach, J. Calculation of the Magnetic Circular Dichroism B Term from the Imaginary Part of the Verdet Constant using Damped Time-dependent Density Functional Theory. *J. Chem. Phys.* **2007**, *127*, 244102.

(10) Solheim, H.; Ruud, K.; Coriani, S.; Norman, P. The A and B Terms of Magnetic Circular Dichroism Revisited. *J. Phys. Chem. A* **2008**, *112*, 9615–9618.

(11) Honda, Y.; Hada, M.; Ehara, M.; Nakatsuji, H.; Downing, J.; Michl, J. Relativistic Effects on Magnetic Circular Dichroism Studied by GUHF/SECI Method. *Chem. Phys. Lett.* **2002**, *355*, 219–225.

(12) Honda, Y.; Hada, M.; Ehara, M.; Nakatsuji, H.; Michl, J. Theoretical Studies on Magnetic Circular Dichroism by the Finite Perturbation Method with Relativistic Corrections. *J. Chem. Phys.* **2005**, *123*, 164113.

(13) Seth, M.; Ziegler, T. Formulation of Magnetically Perturbed Time-dependent Density Functional Theory. *J. Chem. Phys.* **2007**, *127*, 134108.

(14) Seth, M.; Krykunov, M.; Ziegler, T.; Autschbach, J.; Banerjee, A. Application of Magnetically Perturbed Time-dependent Density Functional Theory to Magnetic Circular Dichroism: Calculation of B Terms. *J. Chem. Phys.* **2008**, *128*, 144105.

(15) Seth, M.; Krykunov, M.; Ziegler, T.; Autschbach, J. Application of Magnetically Perturbed Time-dependent Density Functional Theory to Magnetic Circular Dichroism. II. Calculation of A Terms. *J. Chem. Phys.* **2008**, *128*, 234102.

(16) Ganyushin, D.; Neese, F. First-principles Calculations of Magnetic Circular Dichroism Spectra. *J. Chem. Phys.* **2008**, *128*, 114117.

(17) Gendron, F.; Fleischauer, V. E.; Duignan, T. J.; Scott, B. L.; Löble, M. W.; Cary, S. K.; Kozimor, S. A.; Bolvin, H.; Neidig, M. L.; Autschbach, J. Magnetic Circular Dichroism of UCl_6^- in the Ligand-to-Metal Charge-Transfer Spectral Region. *Phys. Chem. Chem. Phys.* **2017**, *19*, 17300–17313.

(18) Heit, Y. N.; Sergentu, D.-C.; Autschbach, J. Magnetic Circular Dichroism Spectra of Transition Metal Complexes Calculated from Restricted Active Space Wavefunctions. *Phys. Chem. Chem. Phys.* **2019**, *21*, 5586–5597.

(19) Solheim, H.; Frediani, L.; Ruud, K.; Coriani, S. An IEF-PCM Study of Solvent Effects on the Faraday $\mathcal{B}$ Term of MCD. *Theor. Chem. Acc.* **2008**, *119*, 231–244.

(20) Khani, S. K.; Faber, R.; Santoro, F.; Hättig, C.; Coriani, S. UV Absorption and Magnetic Circular Dichroism Spectra of Purine, Adenine, and Guanine: A Coupled Cluster Study in Vacuo and in Aqueous Solution. *J. Chem. Theory Comput.* **2019**, *15*, 1242–1254.

(21) Coriani, S.; Hättig, C.; Jørgensen, P.; Helgaker, T. Gauge-origin Independent Magneto-optical Activity within Coupled Cluster Response Theory. *J. Chem. Phys.* **2000**, *113*, 3561–3572.

(22) Kjærgaard, T.; Jansík, B.; Jørgensen, P.; Coriani, S.; Michl, J. Gauge-origin-independent Coupled-Cluster Singles and Doubles Calculation of Magnetic Circular Dichroism of Azabenzenes and Phosphabenzene using London Orbitals. *J. Phys. Chem. A* **2007**, *111*, 11278–11286.

(23) Krykunov, M.; Banerjee, A.; Ziegler, T.; Autschbach, J. Calculation of Verdet Constants with Time-dependent Density Functional Fheory: Implementation and Results for Small Molecules. *J. Chem. Phys.* **2005**, *122*, 074105.

(24) Kjærgaard, T.; Jørgensen, P.; Thorvaldsen, A. J.; Sałek, P.; Coriani, S. Gauge-Origin Independent Formulation and Implementation of Magneto-Optical Activity within Atomic-Orbital-Density Based Hartree- Fock and Kohn- Sham Response Theories. *J. Chem. Theory Comput.* **2009**, *5*, 1997–2020.

(25) Seamans, L.; Linderberg, J. Magneto-optical Activity: Gauge-invariant Calculations in the Random-phase Approximation. *Mol. Phys.* **1972**, *24*, 1393–1405.

(26) Lee, K.-M.; Yabana, K.; Bertsch, G. Magnetic Circular Dichroism in Real-time Time-dependent Density Functional Theory. *J. Chem. Phys.* **2011**, *134*, 144106.

(27) Helgaker, T.; Taylor, P. R. In *Modern Electronic Structure Theory*; Yarkony, D. R., Ed.; World Scientific Publishing Co. Pte. Ltd.: Singapore, 1995; Chapter 12, pp 725–856.

(28) Ding, F.; Liang, W.; Chapman, C. T.; Isborn, C. M.; Li, X. On the Gauge Invariance of Nonperturbative Electronic Dynamics Using the Time-Dependent Hartree-Fock and Time-Dependent Kohn-Sham. *J. Chem. Phys.* **2011**, *135*, 164101.

(29) Lestrange, P. J.; Egidi, F.; Li, X. The Consequences of Improperly Describing Oscillator Strengths Beyond the Electric Dipole Approximation. *J. Chem. Phys.* **2015**, *143*, 234103.

(30) Epstein, S. T. Gauge Invariance of the Hartree-Fock Approximation. *J. Chem. Phys.* **1965**, *42*, 2897–2898.

(31) Epstein, S. Gauge Invariance, Current Conservation, and GIAO's. *J. Chem. Phys.* **1973**, *58*, 1592–1595.

(32) Gauss, J.; Stanton, J. F. Electron-Correlated Approaches for the Calculation of NMR Chemical Shifts. *Adv. Chem. Phys.* **2002**, *123*, 355–422.

(33) Schindler, M.; Kutzelnigg, W. Theory of Magnetic Susceptibilities and NMR Chemical Shifts in Terms of Localized Quantities. II. Application to Some Simple Molecules. *J. Chem. Phys.* **1982**, *76*, 1919–1933.

(34) Kutzelnigg, W. Theory of Magnetic Susceptibilities and NMR Chemical Shifts in Terms of Localized Quantities. *Israel J. Chem.* **1980**, *19*, 193–200.

(35) London, F. Théorie Quantique des Courants Interatomiques dans les Combinaisons Aromatiques. *Journal de Physique et le Radium* **1937**, *8*, 397–409.

(36) Ditchfield, R. Molecular Orbital Theory of Magnetic Shielding and Magnetic Susceptibility. *J. Chem. Phys.* **1972**, *56*, 5688–5691.

(37) Wolinski, K.; Hinton, J. F.; Pulay, P. Efficient Implementation of the Gauge-Independent Atomic Orbital Method for NMR Chemical Shift Calculations. *J. Am. Chem. Soc.* **1990**, *112*, 8251–8260.

(38) Bouten, R.; Baerends, E.; Van Lenthe, E.; Visscher, L.; Schreckenbach, G.; Ziegler, T. Relativistic Effects for NMR Shielding Constants in Transition Metal Oxides Using the Zeroth-Order Regular Approximation. *J. Phys. Chem. A* **2000**, *104*, 5600–5611.

(39) Krykunov, M.; Autschbach, J. Calculation of Origin-Independent Optical Rotation Tensor Components in Approximate Time-Dependent Density Functional Theory. *J. Chem. Phys.* **2006**, *125*, 034102.

(40) Autschbach, J. Analyzing NMR Shielding Tensors Calculated with Two-Component Relativistic Methods Using Spin-Free Localized Molecular Orbitals. *J. Chem. Phys.* **2008**, *128*, 164112.

(41) Helgaker, T.; Jaszuński, M.; Ruud, K. Ab initio Methods for the Calculation of NMR Shielding and Indirect Spin-Spin Coupling Constants. *Chem. Rev.* **1999**, *99*, 293–352.

(42) Helgaker, T.; Coriani, S.; Jørgensen, P.; Kristensen, K.; Olsen, J.; Ruud, K. Recent Advances in Wave Function-Based Methods of Molecular-Property Calculations. *Chem. Rev.* **2012**, *112*, 543–631.

(43) Tellgren, E. I.; Soncini, A.; Helgaker, T. Nonperturbative Ab Initio Calculations in Strong Magnetic Fields using London Orbitals. *J. Chem. Phys.* **2008**, *129*, 154114.

(44) Reynolds, R. D.; Shiozaki, T. Fully Relativistic Self-Consistent Field under a Magnetic Field. *Phys. Chem. Chem. Phys.* **2015**, *17*, 14280–14283.

(45) Irons, T. J.; Zemen, J.; Teale, A. M. Efficient Calculation of Molecular Integrals over London Atomic Orbitals. *J. Chem. Theory Comput.* **2017**, *13*, 3636–3649.

(46) Sen, S.; Tellgren, E. I. Non-perturbative Calculation of Orbital and Spin Effects in Molecules Subject to Non-uniform Magnetic Fields. *J. Chem. Phys.* **2018**, *148*, 184112.

(47) Sun, S.; Williams-Young, D.; Stetina, T. F.; Li, X. Generalized Hartree-Fock with Non-perturbative Treatment of Strong Magnetic Field: Application to Molecular Spin Phase Transition. *J. Chem. Theory Comput.* **2019**, *15*, 348–356.

(48) Li, X.; Williams-Young, D.; Valeev, E. F.; Petrone, A.; Sun, S.; Stetina, T.; Kasper, J. Chronus Quantum, Beta 2 Version. 2018; http://www.chronusquantum.org.

(49) Seth, M.; Autschbach, J.; Ziegler, T. Calculation of the Term of Magnetic Circular Dichroism. a Time-Dependent Density Functional Theory Approach. *J. Chem. Theory Comput.* **2007**, *3*, 434–447.

(50) Becke, A. D. Density-Functional Thermochemistry. III. The Role of Exact Exchange. *J. Chem. Phys.* **1993**, *98*, 5648.

(51) Lee, C.; Yang, W.; Parr, R. G. Development of the Colle-Salvetti Correlation-Energy Formula into a Functional of the Electron Density. *Phys. Rev. B* **1988**, *37*, 785.

(52) Miehlich, B.; Savin, A.; Stoll, H.; Preuss, H. Results Obtained with the Correlation Energy Density Functionals of Becke and Lee, Yang and Parr. *Chem. Phys. Lett.* **1989**, *157*, 200–206.

(53) Hariharan, P. C.; Pople, J. A. The Influence of Polarization Functions on Molecular Orbital Hydrogenation Energies. *Theor. Chem. Acc.* **1973**, *28*, 213–222.

(54) Francl, M. M.; Pietro, W. J.; Hehre, W. J.; Binkley, J. S.; Gordon, M. S.; DeFrees, D. J.; Pople, J. A. Self-consistent Molecular Orbital Methods. XXIII. A Polarization-type Basis Set for Second-row Elements. *J. Chem. Phys.* **1982**, *77*, 3654–3665.

(55) Frisch, M. J.; Trucks, G. W.; Schlegel, H. B.; Scuseria, G. E.; Robb, M. A.; Cheeseman, J. R.; Scalmani, G.; Barone, V.; Petersson, G. A.; Nakatsuji, H.; Li, X.;

Caricato, M.; Marenich, A. V.; Bloino, J.; Janesko, B. G.; Gomperts, R.; Mennucci, B.; Hratchian, H. P.; Ortiz, J. V.; Izmaylov, A. F.; Sonnenberg, J. L.; Williams-Young, D.; Ding, F.; Lipparini, F.; Egidi, F.; Goings, J.; Peng, B.; Petrone, A.; Henderson, T.; Ranasinghe, D.; Zakrzewski, V. G.; Gao, J.; Rega, N.; Zheng, G.; Liang, W.; Hada, M.; Ehara, M.; Toyota, K.; Fukuda, R.; Hasegawa, J.; Ishida, M.; Nakajima, T.; Honda, Y.; Kitao, O.; Nakai, H.; Vreven, T.; Throssell, K.; Montgomery, J. A., Jr.; Peralta, J. E.; Ogliaro, F.; Bearpark, M. J.; Heyd, J. J.; Brothers, E. N.; Kudin, K. N.; Staroverov, V. N.; Keith, T. A.; Kobayashi, R.; Normand, J.; Raghavachari, K.; Rendell, A. P.; Burant, J. C.; Iyengar, S. S.; Tomasi, J.; Cossi, M.; Millam, J. M.; Klene, M.; Adamo, C.; Cammi, R.; Ochterski, J. W.; Martin, R. L.; Morokuma, K.; Farkas, O.; Foresman, J. B.; Fox, D. J. Gaussian16 Revision B.01. 2016; Gaussian Inc. Wallingford CT.

(56) Smith, D.; Williamson, B.; Schatz, P. Identification of the Alkalide, Na-, in Na/NH_3 Matrices using MCD. *Chem. Phys. Lett.* **1986**, *131*, 457–462.

(57) Barth, G.; Bunnenberg, E.; Djerassi, C.; Elder, D.; Records, R. Magnetic Circular Dichroism Studies. Part 10. Investigations of Some Carbonyl Compounds. Symposia of the Faraday Society. 1969; pp 49–60.

Graphical TOC Entry